Recent Advances in Spaceborne Precipitation Radar Measurement Techniques and Technology

Eastwood Im, Stephen L. Durden, Simone Tanelli
Jet Propulsion Laboratory
California Institute of Technology
Pasadena, California, USA
E-mail: eastwood.im@jpl.nasa.gov

Abstract — **NASA is currently developing advanced instrument concepts and technologies for future spaceborne atmospheric radars, with an over-arching objective of making such instruments more capable in supporting future science needs and more cost effective. Two such examples are the Second-Generation Precipitation Radar (PR-2) and the Nexrad-In-Space (NIS). PR-2 is a 14/35-GHz dual-frequency rain radar with a deployable 5-meter, wide-swath scanned membrane antenna, a dual-polarized/dual-frequency receiver, and a real-time digital signal processor. It is intended for Low Earth Orbit (LEO) operations to provide greatly enhanced rainfall profile retrieval accuracy while consuming only a fraction of the mass of the current TRMM Precipitation Radar (PR). NIS is designed to be a 35-GHz Geostationary Earth Orbiting (GEO) radar for providing hourly monitoring of the life cycle of hurricanes and tropical storms. It uses a 35-m, spherical, lightweight membrane antenna and Doppler processing to acquire 3-dimensional information on the intensity and vertical motion of hurricane rainfall.**

I. INTRODUCTION

While the Tropical Rainfall Measuring Mission (TRMM) [1] has provided invaluable data to the user community, it is only the first step towards advancing our understanding of the rain processes and their contributions to weather and climate variability. The follow-on, Global Precipitation Mission (GPM) [2], is currently being developed to capitalize on the information provided by TRMM, and to extend the TRMM's instrument capability to fully address the key science questions from microphysical to climatic time scales. The baseline GPM instrument configuration consists of a constellation of several micro-satellites each carrying a 3-frequency scanning radiometer, and a core satellite which carries a 5-frequency scanning radiometer, and two scanning radars, one operating at 14 GHz and the other at 35-GHz, working in a synchronized and matched-beam fashion. The two radars are intended to provide detailed observations of rainfall processes and microphysics. In order to support the advanced technology development for GPM and other low-earth orbiting (LEO) atmospheric science missions in the future, a notional instrument concept involving a dual-frequency rain radar with a deployable 5-meter electronically-scanned membrane antenna and real-time signal processing has been developed. This new system, the Second Generation Precipitation Radar (PR-2), has the potential of offering greatly enhanced performance at a significantly reduced mass as compared to the TRMM radar.

In a parallel effort, NASA has also initiated an instrument technology definition study on an innovative, geostationary orbiting atmospheric radar, the Nexrad-In-Space (NIS), that can provide detailed monitoring of hurricanes. The observations made with such instrument will enable the four-dimensional hurricane rain and cloud processes to be monitored over much of their life cycle, thus providing the temporal information needed for creating advanced flood and hazard warning systems, improving numerical model prediction of hurricane tracks and landfalls, and understanding more about the hurricane diurnal cycle.

In this paper, the key science rationale and the instrument design concepts for these notional systems will be discussed. Status of the associated technology development will also be presented.

II. PR-2 INSTRUMENT CONCEPT AND TECHNOLOGY

A. PR-2 Design Approach

The PR-2 is designed to operate at orbital altitudes h ranging between 400 and 750 km. It will have two nominal operational modes: the Wide-Swath Mode and the Nadir Doppler Mode. During Wide-Swath mode operations, the antenna will scan ±37° across-track at h = 400 km, or ±28° at h = 750 km. The corresponding ground swaths are 600 and 800 km, respectively. Both the HH-polarized and HV-polarized rain reflectivity profiles at 14 and 35 GHz will be measured simultaneously in this mode. The Nadir Doppler mode will acquire vertical Doppler profiles of precipitation at or near nadir if precipitation is detected in such regions. At 400-km altitude, the required radar antenna aperture size

Sponsors: The Earth-Sun Systems Technology Office (ESTO), the Tropical Rainfall Measuring Mission (TRMM) and the Global Precipitation Measurements (GPM) Mission of NASA.

0-7803-9497-6/06/$20.00 © 2006 IEEE.

is 5.3 m in order to achieve a 2-km horizontal resolution at 14 GHz – the resolution comparable to typical scale size of convective storm cells. The same antenna will be under-illuminated at 35 GHz in order to obtain the matched, 2-km horizontal resolution. When operating at 750 km altitude, the antenna size will be increased to 7.3 m with the corresponding horizontal resolution of ~2.7 km at both frequencies. Similar to that of TRMM PR, the vertical resolution will be 250 m at all altitudes, but the chirp bandwidth will be 5.3 MHz to allow an 8-fold increase in the number of independent samples. The chirp pulse duration will vary in order to ensure sufficient signal-to-noise ratios at all altitudes. The set of PR-2 system parameters are summarized in Table 1.

Table 1. PR-2 system and performance parameters.

Parameter	*h* = 400 Km		*h* = 750 Km	
Frequency (GHz)	14	35	14	35
Antenna effective dia. (m)	5.3	2.1	7.4	2.9
Antenna gain (dBi)	55	55	58	57
Antenna sidelobe (dB)	-30	-30	-30	-30
Peak power (W)	200	50	200	50
Bandwidth (MHz)	5.3	5.3	5.3	5.3
Pulsewidth (μsec)	40	40	40	40
PRF nominal (KHz)	2.7	2.7	2.0	2.0
PRF in Doppler (KHz)	5.0	5.0	5.0	5.0
Vertical resolution (m)	250	250	250	250
Horiz. resolution (Km)	2.0	2.0	2.7	2.7
Ground swath (Km)	600	600	800	800
Independent samples	64	64	64	64
Min. detectable Zeq (dBZ)	5.0	4.8	6.7	5.6
Doppler accuracy (m/s)	1.0	0.9	1.0	0.9

Wide Swath Mode: In this mode, rain reflectivity profiles will be measured over a large cross-track swath using the 'adaptive scan' scheme. The designed antenna scan angle range would cover ground swaths ranging between 600 km at 400 km altitude and 800 km at 750 km altitude. As shown by the GATE results, the probability of rain occurrence over a specific location is < 20%. For this reason, and to effectively utilize the limited observation time, each PR-2 observation sequence will be divided into two periods: a Quick-Scan Period to determine the location and vertical extent of the rain cells within the entire swath, and a Dwell Period at which detailed precipitation measurements of the identified rain cells will be made. For example, at h = 400 km, a nominal observation sequence will last ~0.29 sec, the Quick-Scan Period will occupy the first 0.09 sec and the Dwell Period will use the remaining 0.2 sec. During the Quick-Scan Period PR-2 will make a complete cross-track scan through the 600-km swath, transmit and receive only 1 pulse at each 2-km ground resolution cell at a nominal PRF of 2.7 KHz. The radar backscatter measurements at each resolution cell will be averaged on-board over a vertical column of 2 km (~64 samples) and will be compared with a set of thresholds and ranked according to their respective backscatter strength. The ranked results will then be used to derive the subsequent scan pattern for the Dwell Period. In the Dwell Period, the radar will obtain detailed rain backscatter over areas with significant rainfall. The nominal swath covered in the Dwell Period is ~200 km, which should be sufficient to cover most of the rain areas within the swath. In the event that there is pervasive rainfall covering areas >200 km cross-track, our proposed dwell pattern would allow observations over cells with the most intense rainfall, thus covering a significant portion of the total rainfall in those areas. On-board processing will include pulse compression and range bin averaging.

Nadir Doppler Mode: When the Quick-Scan results indicate rain occurrence at or near nadir, the Nadir Doppler Mode will be exercised. In this mode, the radar antenna will be pointed at this small region for a total time of ~0.05 sec. A higher pulse repetition frequency (~5000) will be used to accommodate the anticipated Doppler spread. Multiple rain echoes obtained in each resolution cell will be used to estimate the Doppler shift caused by the mean rainfall motion. The mean vertical rainfall motion can be measured to an accuracy of about 1 m/s.

B. PR-2 Radio-Frequency Electronics

The PR-2 RF electronics subsystem consists of a NCO-based digital chirp generator (DCG) to synthesize the chirp waveforms, an upconverter and four receiver channels. The DCG approach has allowed flexibility in generating the shaped, linearly frequency-modulated pulses with sidelobe levels below -60 dB [3]. The chirp waveform is generated at an IF frequency and upconverted to both 14 and 35 GHz using a two-stage mixing process. The LO frequencies are provided by phase-locked oscillators and dielectric resonator oscillators, which are locked to a reference oscillator for coherent up- and down-conversion, as is required for the Doppler mode. The signals are amplified to the desired radiated powers using the 14 and 35 GHz TWTAs and transmitted through an ortho-mode transducer (OMT) and a circulator assembly to the antenna. The OMT and circulator are used to separate the horizontal and vertical polarization components at each frequency. A small amount of power in the transmit pulse is also directly coupled to the receiver channels to calibrate the sensitivity of the system and to accurately measure receiver gain and noise floor. There are four receiver channels, two required for 14 GHz (H- and V-pol) and two for 35 GHz (H- and V-pol). The receiver amplifies the returned echo using a low noise amplifier and coherently down-converts the signal to offset video.

The PR-2 LO/IF module is designed to be compact and flight qualifiable. Its prototype model as shown in Fig. 1 fits in two VME card slots and weighs 3.6 kg. Owning to its compact configuration, it is easily accessible for serviceability during testing, and is easy to be reconfigured for use by multiple missions. It has very good EMC characteristics with thorough sub-circuit shielding, and is conduction-cool.

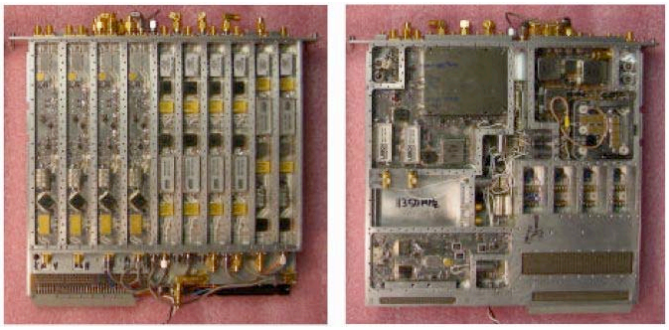

Figure 1. Front- and back-side of the PR-2 LO/IF module.

C. PR-2 Digital Electronics and Real-Time Processor

The PR-2 digital electronics subsystem consists of the control and timing unit, analog-to-digital converters (ADCs) for the four receiver channels, multiplexer, data processor, and data formatter. The control and timing unit decodes all radar commands, generates timing signals, and controls the antenna beam scan timings. The digitized data output from the ADCs are multiplexed and sent to the real-time processor. The processor performs digital pulse compression, range bin averaging, ranking of the Quick-Scan data to determine rain locations, and Doppler processing. The processed data are formatted and sent to the tape recorder for storage.

The PR-2's real-time digital pulse compression technology has been demonstrated by the development of the airborne prototype model. This model uses a combination of custom and commercial-off-the-shelf (COTS) VME hardware. The system has two main components, a four-channel (two received polarizations by two frequencies) acquisition board and a programmable digital signal processor board which uses Xilinx field programmable gate arrays (FPGAs).

The real-time signal processor card shown in Fig. 2 is a COTS VME card made by Annapolis Microsystems. The board contains three large Xilinx Vertex FPGAs; reprogrammable parts which can be configured as almost any kind of digital logic. With four channels, the system performs 20 billion multiplications and 20 billion additions per second. This processing throughput would be difficult to achieve with microprocessors. The highly parallel implementations possible with FPGAs allow realization of the entire real-time processor in only two chips. The front-end of the processor is four 64-tap, 16-bit finite impulse response (FIR) filters implemented with bit serial multipliers clocking at 133 MHz. Following the filter is a downsampling and digital IQ demodulation yielding in-phase and quadrature baseband signals. A Kaiser window (K=6) squared envelope modulated on an ideal chirp is used as the reference function.

The PR-2 prototype's pulse compression performance was evaluated during an airborne engineering test flight in which the nadir returns from the clear ocean were captured and processed in real time. Fig. 3 shows an example of the processor output signals (an average of 64 individual pulses). This figure demonstrates that the technique can indeed achieve sidelobe suppression of 60 dB as designed.

Figure 2. FPGA-based PR-2 data processor.

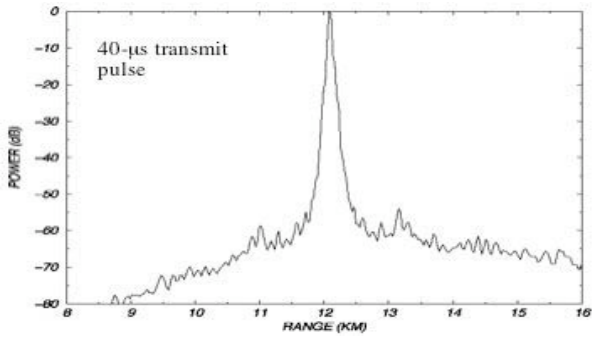

Figure 3. Compressed signal wavefrom from clear ocean.

D. PR-2 Dual-Frequency Membrane Antenna

The large swath coverage and fine horizontal resolution desired for detailed rain profiling by radars lead to the use of a large (5 to 7 m diameter), dual-frequency, scanning antenna. In order to achieve the goals of low antenna mass and small stowage volume, the PR-2 antenna design is a cylindrical/ parabolic membrane reflector offset-fed by two linear feed arrays, one at each frequency, with T/R modules and phase shifters [4]. Singly curved reflector as designed allows the main beam to scan over a wider angular range in one (cross-track) dimension. Linear array feeds are used because they only require N T/R modules instead of $N \times N$ as required for the planar arrays. An offset configuration is selected to avoid feed blockage and, thus, to achieve the required low sidelobe level. In order to achieve matched beams at the two frequencies, the 35-GHz feed will under-illuminate the reflector and be less than half the length of the 14-GHz feed.

The PR-2 antenna's mechanical configuration comprises a parabolic cylindrical membrane reflector supported by a rigid mandrel at the top, a rigid feed array interface at the bottom, and two sets of precision chain links, one at the left and one at the right side, of the curved membrane boundaries. Each chain link set is supported by a inflatable and rigidizable tube boom, which provides precision deployment, pre-tension, and shape maintenance of the reflective membrane. The tube boom and chain link structure are cantilevered from the array feed interface and

interconnected at their free ends by the same rigid mandrel. At stow, each chain link/boom, together with the reflective membrane, are rolled up around the mandrel, thus forming a cylindrical bundle. This antenna design is expected to have a mass density of less than 2.5 kg/m^2. In order to meet the low sidelobe requirement, the antenna's RMS surface accuracy should be better than 0.25 mm. To maintain such accuracy, the antenna must strive for a deployed fundamental frequency $\geq$ 0.5 Hz, the inflatable tube must be rigidized, and the reflective membrane must be dimensionally stable through the entire mission life in the expected space environments.

In order to assess the technical feasibility of such design, a half-size (2.6 m x 2.6 m) PR-2 antenna prototype model was built and tested in 2004. Fig. 4(a) shows the membrane reflector rested on the support structure, and Fig. 4(b) shows the chain-link set during a deployment test. The laser metrology measurements show that this prototype was only able to achieve a 2-mm RMS accuracy, which exceeded the requirement by a factor of 8. As the result, the subsequent antenna pattern measurements indicated much higher sidelobe levels than required, with peak sidelobe reaching -13 to -15 dB at both frequencies (see Fig. 5). The computer-simulated patterns based on surface metrology measurements reproduced the observed RF patterns reasonably well.

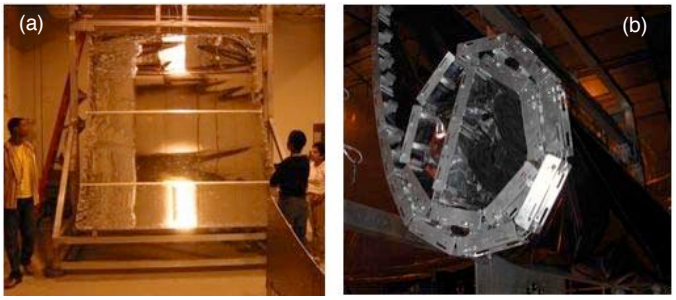

Figure 4. Half-size prototype model of the PR-2 antenna: (a) membrane reflector surface; (b) chain-link set during deployment test.

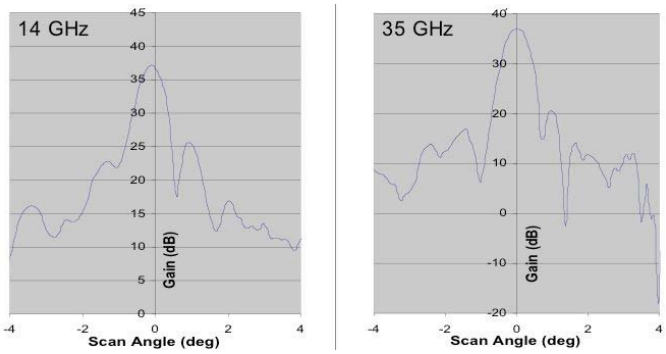

Figure 5. The measured RF antenna pattern of the PR-2 antenna prototype model at 14 GHz (l) and 35 GHz (r).

The degraded performance on the antenna prototype was caused by several factors, including gravity-induced surface sag; surface ripples resulted from non-uniform tension at the boundary interfaces, size of individual chain links, and manufacturing imperfection. Despite these challenges, the first prototype of this new technology suggests that the design concept is promising, and that the manufacturing and testing processes require substantial improvement.

III. NIS Instrument Concept and Technology

Concurrent to the LEO atmospheric radar study, the instrument concept and the associated technology roadmap for a notional GEO atmospheric radar are also being developed by NASA. The objective of the technology roadmap is to make use of the LEO PR-2 type technology to the extent possible, and at the same time identify additional technology items that are unique and necessary for the eventual implementation of such a geostationary radar flight instrument.

The advantage of a space radar's ability to penetrate precipitating clouds relative to standard GOES cloud imagery is illustrated in Fig. 6. This figure emphasizes how TRMM PR information can be used quantitatively to gauge the intensity of a hurricane, its vertical rain rate structure, and its water carrying capacity. It is also evident that the complete and frequent hurricane coverage by a geo-profiling radar will enable hurricane rain and cloud processes to be monitored over much of their life cycle, thus providing the temporal information needed for creating advanced flood and hazard warning systems, improving numerical model prediction of hurricane tracks and landfalls, and understanding more about the hurricane diurnal cycle. Geostationary radar measurements, when used together with existing GOES measurements, can deduce vertical and horizontal cloud structure for the study and monitoring of solar and infrared radiative transfer in heterogeneous cloudy atmospheres, the essential ingredients for accurate diagnosis of the Earth's radiation budget and the atmosphere's radiative heating-cooling behavior. Since this radar approach is analogous to putting a NEXRAD (NEXt generation RADar) system in orbit, it is being referred to as "NEXRAD-in-Space (NIS)".

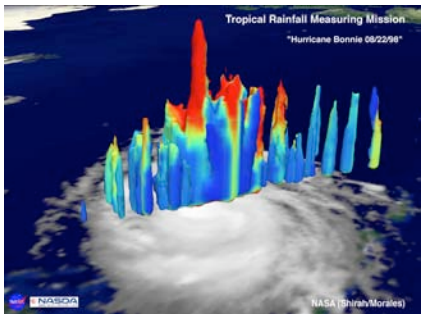

Figure 6. TRMM PR acquired vertical rain profiles of Hurricane Bonnie overlaid on the corresponding GOES image.

A. NIS Design Approach and Observational Concept

NIS is designed to operate in a geostationary orbit at an altitude of 36,000 km. From the trade study between spatial resolution and rain penetration/profiling, we have selected 35 GHz as the radar frequency. A deployable, 35-m, spherical

antenna reflector will be used together with two pairs of antenna feeds to form the overall antenna subsystem. Each pair of antenna feeds will consist of one for signal transmission and the other for echo reception. The transmit/receive dual-feed approach is used to compensate for the long range distance. The angular spacing between the transmit and receive feeds is designed to be 0.45˚ such that the rain echoes can be captured 0.25 seconds after pulse transmission. Both the reflector and the spacecraft will remain stationary as the antenna feeds perform spiral scans up to 4˚ from boresight to cover a 5300-km circular disk on the Earth surface. This coverage is equivalent to 48˚ (±24˚) in both longitude and latitude. If necessary, small spacecraft maneuvers can be used to extend the latitudinal coverage. This scan approach allows continuous and smooth transition between adjacent radar footprints. The NIS surface coverage is graphically illustrated in Fig. 7. The corresponding horizontal resolution ranges from 12 km at nadir to 14 km at 4˚ scan.

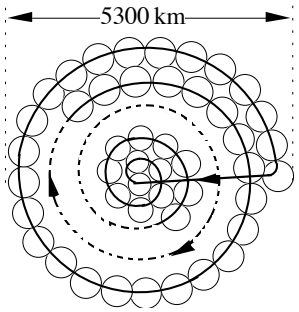

Figure 7. Surface coverage by the spiral scan pattern.

Table 2. NIS systems and performance parameters.

Radar System Parameters			
Frequency	35 GHz	Time for a full scan	60 mins.
Antenna diameter	35 m	Peak power	100 W
Ant. effective aperture	28 m	Pulsewidth	25 μs
Ant. 3-dB beamwidth	0.019˚	PRF	3.5 - 7 KHz
Antenna gain	77.2 dBi	Power duty cycle	35%
Antenna sidelobe	-30 dB	Sys. Noise temp.	910 K
Max. spiral scan angle	4˚	Dynamic range	70 dB
Performance Parameters			
Disk coverage diameter	5300 Km	Vertical resolution	300 m
Horiz. resolution (nadir)	12 Km	Min. Zeq (after ave)	< 10 dBZ
Horiz. resolution (4˚)	14 Km	Doppler precision	0.3 m/s

The key NIS instrument and performance parameters are summarized in Table 2. Like all downward pointing precipitation radars, the NIS return signals from light rain can be contaminated by the simultaneous surface returns when the antenna is scanned away from nadir. However, since the rain rates associated with hurricanes and the 35-GHz rain attenuation are high, the surface clutter contamination is much less an issue than one might expect. To articulate this point, we computed the ratios of the rain signal to the combined noise and clutter SNCR) at different rain rates. An example at 5 mm/hr rain over the ocean is shown in Fig. 8. The results show that at 5 mm/hr rain NIS can indeed penetrate down to lower than 2 km altitude at most incidence angles of interest. At larger rain rates the detectability is determined by attenuation and thermal noise, not clutter.

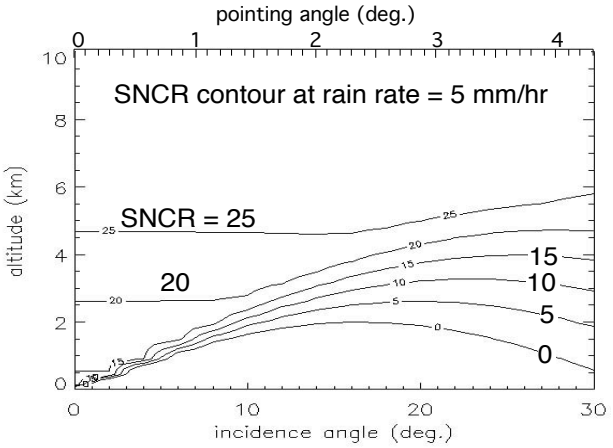

Figure 8. SNCRs for the NIS at 5 mm/hr rain.

B. NIS Electronics

The NIS electronics design and functions are intended to mimic those of the PR-2 in order to leverage off the PR-2 electronics technology currently being developed. It consists of the RF electronics, digital electronics, and on-board processor. Since NIS requires only one transmitter and one receiver at 35 GHz, the functional requirements on the RF/digital electronics, as well as for the processor, will be significantly reduced. As such, the technology developed for the PR-2 electronics can be applied directly to NIS.

C. NIS Antenna Approach

NIS antenna requirements include an antenna gain of 77 dB, a beamwidth of 0.02˚, a sidelobe level of lower than -30 dB, and a scan of up to 4˚ off its axis. This angular scan translates into a scan of ±200 beamwidths. After an extensive trade study, we have focused on a novel spherical reflector antenna design [5] which is capable of scanning its beams to any desired direction without compromise on the radiation performance. Any spherical aberration-induced degradation will be overcome by using a small planar array in the focal plane. Such a focal array can achieve any desired beam direction; more importantly, there is no need to reconfigure the array excitation coefficients for new beam direction.

Spherical reflector antennas produce almost identical beams when their feeds are rotated with respect to the focal point. The major drawback is the excessive gain loss due to the presence of an extended focal region. Since the objective is to cover a ±4˚ angular range, an oversized, 35-m reflector antenna is used to cover the desired angular range by

utilizing sub-apertures for various beam look angles. Our initial parametric study showed that the utilization of a 271-element, rotating, fixed feed array with complex excitation coefficients would substantially improve the performance of the spherical reflector antenna. The size of the feed array is ~20 cm in diameter. The corresponding antenna radiation patterns at 4˚ scan are shown in Fig. 9. Note that an antenna gain of ~80 dB with sidelobe levels below 30 dB are obtained.

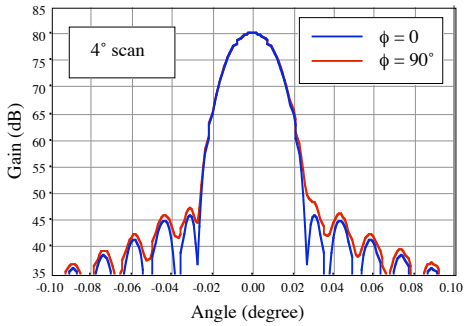

Figure 9. NIS antenna patterns at 4˚ off-axis.

The two pairs of feed arrays will be mechanically moved on two interleaved spiral tracks. The mechanism approach we are implementing is a rotating arm, pivoting around its center. The rotating arm carries two trolleys each containing one feed pair. The two trolleys travel along the axis of the arm (on opposing sides) on precision wheels preloaded against precision rails. This scanning mechanism approach, as graphically illustrated in Fig. 10, allows the balancing of the torque due to rotation. It also cut the rate of rotation by half. Because of the slower scan rate, the radar dwell time will be double, resulting in a two-fold increase in the number of radar echo samples obtained, which translates into a factor of 1.4 reductions in measurement noise.

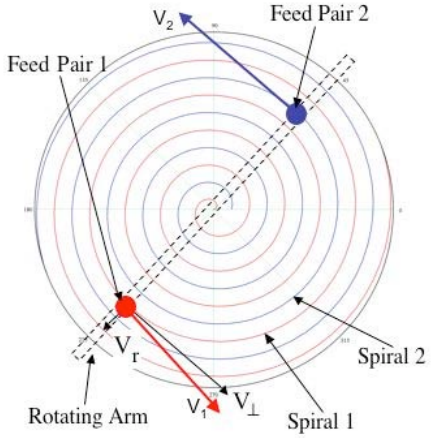

Figure 10. The NIS antenna feed scanning mechanism approach.

From mass and size considerations, three mechanical reflector concepts can potentially be adapted for the NIS antenna application. The first concept, shown in Fig. 11(a), employs the emerging space inflatable technology. When deployed, the reflector assumes a lenticular shape formed by two spherical thin-film membrane halves. One of the membrane halves is coated and functions as the reflective surface. The other membrane half is a transparent canopy, with the sole function of holding the extremely low (about 10^{-4} psi) inflation pressure. A circular torus and three struts, all are made of membrane materials and are inflation deployable and space rigidizeable, provide structural support for the reflector. Ultra-flex solar arrays that have membrane substrates can be mounted on the surface of the torus. Development of flexible solar arrays with higher efficiency is currently being carried out mainly under the sponsorship of DoD. Based on ground measurements of a 14-m off-axis parabolic reflector developed for the Inflatable Antenna Experiment (IAE) launched with the shuttle mission in 1996, the best as-manufactured surface accuracy for an on-axis spherical inflatable reflector is expected to be in the range of 0.5 to 1 mm RMS. To further improve the surface accuracy, adaptive shape control can be used for on-orbit configuration adjustments.

The second design concept in Fig. 11(b) uses the AstroMesh reflector approach. Structurally, this reflector consists of a cable-actuated synchronized parallelogram mechanism (that deploys the reflector) and a pair of ring-stiffened, tension-tied geodesic domes. The reflective mesh is stretched over the back of one of the domes. Based on the measured surface error of < 0.36 mm RMS on the Astro's 6-m flight model, and the consideration on several potential design improvements, including denser geodesic net structures, CTE tailoring, thinner webs, and refined materials conditioning, a 30-m AstroMesh reflector should meet the 0.75-mm RMS performance goal. Since sunrays can pass the mesh, traditional solid solar array panels attached to the spacecraft bus can be used for this option.

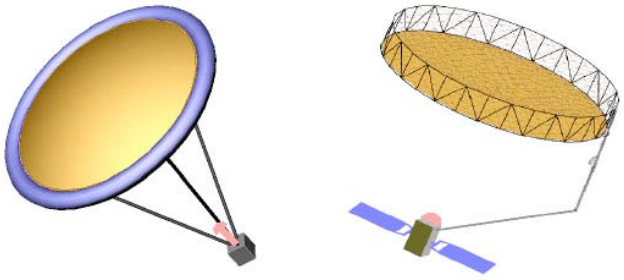

Figure 11. (a) Inflatable reflector concept; (b) AstroMesh concept.

The third concept option is a hybrid of the first two concepts. It uses the mesh to deploy a reflective thin-film (less than 1 mil) antenna aperture for improved RF performance. In this case, the mesh can be made of thin lightweight wires and the grids of the mesh can be relatively course. With a slightly increased reflector diameter, an annular ring of ultra-flex membrane solar arrays can be

incorporated around the antenna aperture to eliminate the need for traditional solid solar panels.

IV. SUMMARY

This paper presents the conceptual designs and the technologies associated with the next-generation of atmospheric radars for remote sensing of precipitation from both the low-earth and geostationary orbits. In each case, several innovative design and technology features are being incorporated in order to enhance the rain measurement capability.

For the low earth orbiting PR-2 instrument, these innovative features include: 14/35-GHz dual-frequency operations, a large, shared-aperture, deployable, scanning antenna, dual-polarization, nadir Doppler measurements, pulse compression and real-time data processing, and instrument flexibility. It is anticipated that such instrument concept can provide significant data for advancing our understanding on rain processes, latent heating, climate variability, and atmospheric anomalies.

For the geostationary earth orbiting NIS instrument concept, the innovative features include a 35-GHz spirally scanning antenna feed set and a large, deployable spherical membrane antenna reflector. These combined features allowed the NIS instrument to acquire detailed information of the 3-dimensional structures of hurricanes, cyclones, and severe storms once every hour at 13-km horizontal resolution, 300-m vertical resolution, and 0.3-m/s precision in line-of-sight Doppler velocity.

ACKNOWLEDGMENT

The research described in this paper was performed at the Jet Propulsion Laboratory, California Institute of Technology, under contract with the National Aeronautics and Space Administration (NASA). The authors would like to acknowledge the supports provided by the Earth-Sun System Technology Office (ESTO), the Tropical Rainfall Measuring Mission (TRMM) and the Global Precipitation Measurements (GPM) Mission of NASA.

REFERENCES

[1] C. Kummerow, et al., "The status of the Tropical Rainfall Measuring Mission (TRMM) after 2 years in orbit," J. Appl. Meteor., vol. 39, pp. 1965-1982, 2000.

[2] E.A. Smith, W.J. Adams, G.M. Flaming, S.P. Neek, and J.M. Shepherd, "The Global Precipitation Measurement (GPM) mission," Mediterranean Storms 2001 (edited by R. Deidda, A. Mugnai, and F. Siccardi), pp. 175-183, 2002.

[3] S. L. Durden, E. Im, F.K. Li, W. Ricketts, A. Tanner, and W. Wilson, "ARMAR: An airborne rain mapping Radar," J. Atmos. Oceanic Technol., vol. 11, pp. 727-737, 1994.

[4] Y. Rahmat-Samii, Y., J. Huang, B. Lopez, M. Lou, E. Im, S.L. Durden, and K. Bahadori, "Advanced Precipitation Radar Antenna: Array-fed fffset membrane cylindrical reflector antenna," IEEE Trans. Ant. and Propag., vol. 53, 2503-2515, 2005.

[5] Y. Rahmat-Samii, "Improved reflector antenna performance using optimized feed arrays," Proc. of 1989 URSI Intl. Sympos. on Electromagnetic Theory, pp. 559-561, Stockholm, Sweden, August 14-17, 1989.